chemosensors

Review

Autonomous Oscillation of Nonthermoresponsive Polymers and Gels Induced by the Belousov–Zhabotinsky Reaction

Yusuke Hara

Nanosystem Research Institute, NRI, National Institute of Advanced Science and Technology, AIST, Central 5-2, 1-1-1 Higashi, Tsukuba 305-8565, Japan; E-Mail: y-hara@aist.go.jp; Tel.: +81-29-861-9318; Fax: +81-29-81-6236

Abstract: This review introduces the self-oscillating behavior of two types of nonthermoresponsive polymer systems with Ru catalyst moieties for the Belousov-Zhabotinsky (BZ) reaction: one with a poly-vinylpyrrolidone (PVP) main chain, and the other with a poly(2-propenamide) (polyacrylamide) (PAM) main chain. The amplitude of the VP-based self-oscillating polymer chain and the activation energy for self-oscillation are hardly affected by the initial concentrations of the BZ substrates. The influences of the initial concentrations of the BZ substrates and the temperature on the period of the swelling-deswelling self-oscillation are examined in detail. Logarithmic plots of the period against the initial concentration of one BZ substrate, when the concentrations of the other two BZ substrates are fixed, show good linear relationships. The period of the swelling-deswelling self-oscillation decreases with increasing temperature, in accordance with the Arrhenius equation. The maximum frequency (0.5 Hz) of the poly(VP-*co*-Ru(bpy)$_3$) gel is 20 times that of the poly(NIPAAm-*co*-Ru(bpy)$_3$) gel. It is also demonstrated that the amplitude of the volume self-oscillation for the gel has a tradeoff with the self-oscillation period. In addition, this review reports the self-oscillating behavior of an AM-based self-oscillating polymer chain as compared to that of the VP-based polymer chain.

Keywords: BZ reaction; gel; polymer chain; actuator; autonomous; self-oscillation

1. Introduction

Intelligent materials with changing properties and functions have been studied in many fields [1–10]. Recently, molecular devices fabricated by taking advantage of DNA base sequences have been much investigated, because molecular programming can be performed by utilizing DNA [11–16]. With DNA base sequences, 2D and 3D DNA nanostructures in solution based on rigid motifs including several DNA junctions and building blocks can be designed. In addition, stimuli-responsive polymer systems have been studied for many possible applications, such as soft actuators, chemical robots, microfluidics, medical devices, *etc.*, because of their light weight, flexibility, low-noise operation, *etc.* [17–22]. Gel actuators have been considered for applications in biomimetic robots and soft actuators, because gels simultaneously have flexible bodies allowing volume changes as well as chemical-substance-sensing properties. In particular, the thermoresponsive poly(N-isopropylacrylamide) (PNIPAAm) gel has been much studied, especially for medical devices [23,24]. One drawback of these materials is that external devices for controlling the external stimulus are needed to drive their transformations. In contrast, living organisms can generate autonomous motion without external stimuli. Thus, if autonomous polymer actuators like living organisms are realized, unprecedented actuators and robots could be constructed.

In previous investigations, an autonomous polymer system that converts chemical energy to mechanical work through the Belousov-Zhabotinsky (BZ) reaction was developed [25–27]. The BZ reaction has been extensively studied both experimentally and theoretically, because it can be treated as a simple model for the formation of a spatiotemporal structure such as a spiral pattern or a target pattern in an unstirred solution, and because it exhibits multistability, periodicity, and/or multiperiodicity in a stirred solution [28–38]. The overall process of the BZ reaction is the oxidization of an organic substrate by an oxidizing agent in the presence of the catalyst under strong acidic conditions. In the BZ reaction, the oxidation number of the ruthenium tris (2,2′-bipyridine), *i.e.*, the metal catalyst of the BZ reaction, undergoes periodic changes. At the same time, the solubility of the Ru catalyst also changes periodically. In order to synchronize the periodic changes in the solubility of the metal catalyst with the solubility of a polymer, polymer systems covalently bonded to the Ru catalyst were synthesized. The polymer chain with the Ru catalyst moiety undergoes aggregation-disaggregation self-oscillation induced by the BZ reaction without external stimuli. Thus, the gel with the Ru catalyst exhibits swelling-deswelling self-oscillation without external stimuli.

To improve the functions of self-oscillating polymer systems, Hara *et al.* synthesized a novel self-oscillating polymer system consisting of *N*-isopropylacrylamide (NIPAAm), the Ru catalyst, and a negatively charged acrylamide-2-methylpropanesulfonic acid (AMPS) as a pH and solubility control site [39–42]. The AMPS-containing self-oscillating polymers exhibit novel self-oscillating behavior and can be used to fabricate novel autonomous actuators. By utilizing AMPS-containing polymer chains, novel phenomena such as on-off switching of the self-oscillation and viscosity self-oscillation for high-concentration AMPS-containing polymer solutions were achieved [43,44]. Moreover, by utilizing AMPS-containing polymer gels, a self-walking gel robot and a matter transport gel system were constructed [45–47]. However, these self-oscillating polymer systems have limited temperature ranges for the self-oscillation because of the thermoresponsive nature of the poly(NIPAAm) main

chain. These temperature limitations of the self-oscillating system are a big problem for the design of many types of autonomous actuators and robots.

This review introduces novel self-oscillating polymer systems consisting of nonthermoresponsive polymer main chains that were developed in order to expand the field of applications of self-oscillating polymer systems. In previous reports, Hara *et al.* described various types of self-oscillating polymer systems with nonthermoresponsive main chains. Among them, we selected poly-vinylpyrrolidone (PVP) [48–52] and poly(2-propenamide) (polyacrylamide) (PAM) [53–55] for discussion here. As for the VP-based self-oscillating polymer chain, the influence of the concentrations of the three BZ substrates (sodium bromate, malonic acid, and nitric acid; not including metal catalyst) on the waveform and period of the self-oscillation was investigated. It was demonstrated that the amplitude of the self-oscillation is hardly affected by the initial concentration of the BZ substrates. In addition, the activation energy of the aggregation–disaggregation self-oscillation was evaluated over broad concentrations of the three BZ substrates in a wide temperature range. This is of interest because the activation energy cannot be evaluated for conventional self-oscillating polymer systems in wide temperature ranges because of the existence of the lower critical solution temperature (LCST). Furthermore, Nakamaru *et al.* first succeeded in undergoing the swelling-deswelling self-oscillation at a high temperature by adapting the VP-based polymer main chain. In this study, the influence of the initial concentrations of the three BZ substrates (not including the metal catalyst) on the period of the self-oscillation of the gel was reported, along with the influence of temperature. By optimizing the initial concentration of the BZ substrates and the temperature, it was demonstrated that the maximum frequency of the swelling-deswelling self-oscillation for the gel is 0.5 Hz. This value is 20 times that of the conventional self-oscillating poly(NIPAAm-co-Ru(bpy)$_3$) thermoresponsive gel. However, the mechanical strength of the VP-based polymer gel is too weak for many types of actuators, robots, and so on. Therefore, in order to improve the mechanical strength of the self-oscillating polymer system, PAM was selected as the main chain of a self-oscillating polymer system. In this review, I introduce the self-oscillating behavior and activation energy for the AM-based self-oscillating polymer chain.

2. Experimental Section

2.1. Polymerization of Poly(VP-co-Ru(bpy)$_3$)

The poly(VP-co-Ru(bpy)$_3$) (Figure 1) was prepared as follows. First, 0.5 g of ruthenium(4-vinyl-4′-methyl-2,2′-bipylridine)bis(2,2′-bipyridine)bis(hexafluorophosphate) (Ru(bpy)$_3$) as a metal catalyst for the BZ reaction, 9.5 g of vinylpyrrolidone (VP), and 0.35 g of 2,2′-azobis(isobutyronitrile) (AIBN) as an initiator were dissolved in a methanol solution (31 g) with a total monomer concentration of 20 wt%. These polymerizations were carried out at 60 ℃ for 24 h *in vacuo*. The resulting reaction mixtures were dialyzed against graded series of water/methanol mixtures for 1 day each in 0, 25, 50, 75, and 100 wt% water and then freeze-dried.

Figure 1. Chemical structure of poly(VP-*co*-Ru(bpy)$_3$).
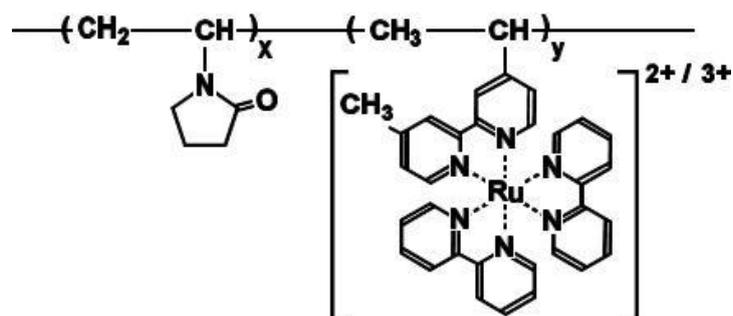
2.2. Synthesis of Poly(VP-co-Ru(bpy)$_3$) Gel

The poly(VP-co-Ru(bpy)$_3$) gel (Figure 2) was prepared as follows. First, 0.11 g of Ru(bpy)$_3$ as a metal catalyst for the BZ reaction was dissolved in 0.877 g of vinylpyrrolidone (VP). Then, 12 mg of *N,N'*-methylenebisacrylamide (MBAAm) as a cross-linker and 20 mg of 2,2′-azobis(isobutyronitrile) (AIBN) as an initiator were dissolved in the methanol solution (3 mL). The two solutions were mixed together well, and then the mixed solution was purged with dry nitrogen gas. The monomer solution was injected between Teflon plates separated by silicone rubber as a spacer (thickness: 0.5 mm) and then polymerized at 60 ℃ for 18 h. After gelation, the gel strip was soaked in pure methanol for a week to remove unreacted monomers. The gel was carefully hydrated by dipping it in a graded series of methanol-water mixtures for 1 day each in 75, 50, 25, and 0 wt% water.

Figure 2. Chemical structure of poly(VP-*co*-Ru(bpy)$_3$) gel.
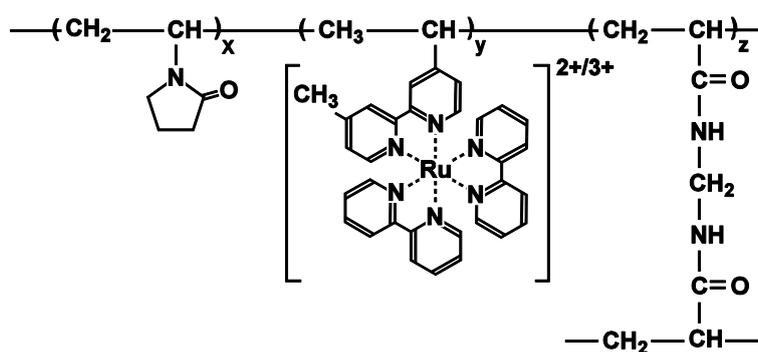
2.3. Polymerization of Poly(AM-co-Ru(bpy)$_3$)

The poly(AM-co-Ru(bpy)$_3$) (Figure 3) was synthesized by radical polymerization in ethanol (47.8 g) under a total monomer concentration of 10 wt%, using acrylamide monomer (AM) (4.54 g), Ru(bpy)$_3$ (0.58 g), and 2,2′-azoisobutyronitrile (AIBN) (0.32 g) as an initiator. These polymerizations were carried out at 60 ℃ for 24 h *in vacuo*. The resulting reaction mixtures were dialyzed against a graded series of water-ethanol mixtures for 1 day each in 0, 25, 50, 75, and 100 wt% water and then freeze-dried.

Figure 3. Chemical structure of poly(AM-*co*-Ru(bpy)$_3$).
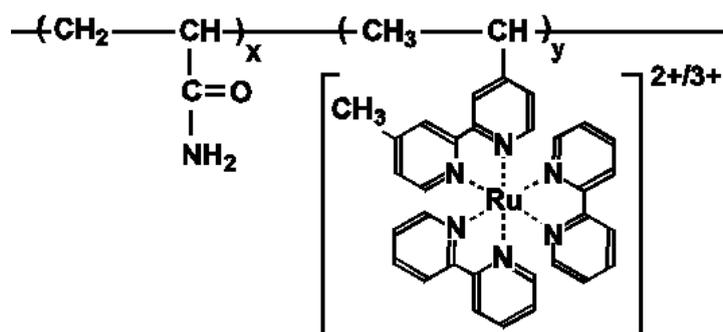
2.4. Measurement of Lower Critical Solution Temperature (LCST)

The LCST of the polymer solution was measured under the reduced and oxidized states by using Ce(SO$_4$)$_2$ as an oxidizing agent and Ce$_2$(SO$_4$)$_3$ as a reducing agent. The polymer solutions were prepared by dissolving the polymer in a 0.3 M HNO$_3$ aqueous solution and adding 5 mM Ce(SO$_4$)$_2$ or 5 mM Ce$_2$(SO$_4$)$_3$. The LCST measurements were carried out with a spectrophotometer (JASCO, Model V-630, Tokyo, Japan) equipped with magnetic stirrers and a thermostatic controller. In this measurement, the 570 nm wavelength was used because it is the isosbestic point for the reduced and oxidized states of Ru(bpy)$_3$. The transmittance (%) of the polymer solution at 570 nm was then recorded by raising the temperature at the rate of 0.5 °C/min.

2.5. Measurement of Optical Transmittance Self-Oscillations

The polymer solutions were prepared by dissolving the polymer into an aqueous solution containing the three BZ substrates (malonic acid (MA), sodium bromate (NaBrO$_3$), and nitric acid (HNO$_3$)). The measurements of the transmittance self-oscillation were carried out with a spectrophotometer (JASCO, Model V-630, Tokyo, Japan). The self-oscillations of the polymer solutions were measured under constant temperature with stirring. In order to detect the transmittance change, a wavelength of 570 nm was used. The time series of the transmittance at 570 nm was monitored by a spectrophotometer.

2.6. Measurement of Equilibrium Swelling Ratio of Poly(VP-co-Ru(bpy)$_3$) Gels

The equilibrium swelling ratio of the gels in the reduced and the oxidized states was measured by using the oxidizing and reducing agents. Gels were added to either Ce(III) solution with [Ce$_2$(SO$_4$)$_3$] = 0.001 M and [HNO$_3$] = 0.3 M or Ce(IV) solution with [Ce$_3$(SO$_4$)$_2$] = 0.001 M and [HNO$_3$] = 0.3 M, both of which had the same acidity. The equilibrium swelling ratio of the gels was observed and recorded using a microscope (Fortissimo Corp. WAT-250D, Tokyo, Japan), an LED light (LEDR-74/40 W), and a video recorder (Victor Corp. SR-DVM700, Tokyo, Japan). Analysis was conducted using image processing software (Image J 1.38x). Measurements of the equilibrium swelling ratio were performed in a water-jacketed cell made of acrylic plates.

*2.7. Investigation of Oscillating Behavior of Poly(VP-*co*-Ru(bpy)₃) Gel*

The gel membrane was cut into rectangles (side length about 2×20 mm) and immersed into 8 mL of an aqueous solution containing malonic acid (MA), sodium bromate (NaBrO₃), and nitric acid (HNO₃). Changes in the shape of the gel strip were observed and recorded using a microscope (OLYMPUS.IX71, Tokyo, Japan) and a video recorder (Victor Corp. SR-DVM700, Tokyo, Japan). Analysis was conducted using image processing software (Image J 1.38x). A one-pixel line along the length of the recorded gel image was stored at regular time intervals (0.05 s). The stored pixel line images were sequentially lined up as a function of time by the computer, to construct a spatiotemporal diagram. From the obtained diagram, the time-dependent change in the gel edge was traced in order to show the volume change behavior.

3. Results and Discussion

The LCSTs of the poly(VP-*co*-Ru(bpy)₃) solution in the reduced and oxidized states were measured for by changing the temperature. It was demonstrated that there was no LCST for the VP-based polymer chain in the reduced and oxidized states (see Figure 4) [49]. The solubility of the VP-based polymer chains was different in the reduced and oxidized states, as evidenced by the different transmittance values. Thus, the difference in solubility drives the transmittance self-oscillation under constant-temperature conditions. The NIPAAm-based self-oscillating polymer chain is more soluble in the oxidized state than in the reduced state, whereas as shown in Figure 4, the solubility of the VP-based polymer solution is higher in the reduced state than in the oxidized state [26,39,40]. This difference can be attributed to the chemical structure of the VP main chain.

> **Figure 4.** Temperature dependence of transmittance of poly(VP-*co*-Ru(bpy)₃) solutions under the reduced Ru(II) (in Ce(III) solution) and oxidized Ru(III) (in Ce(IV) solution) states.
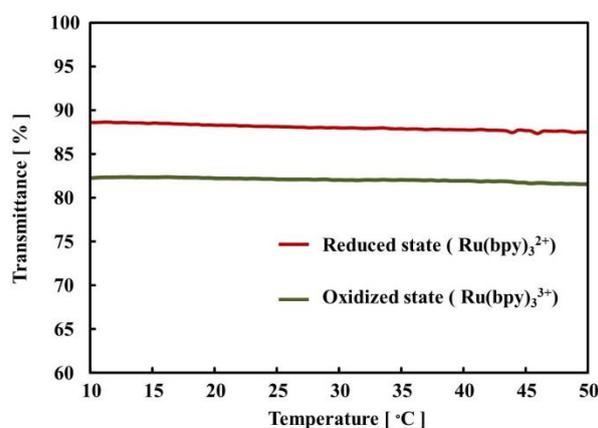
As shown in Figure 5, the VP-based polymer chain undergoes transmittance self-oscillation originating from the aggregation-disaggregation of the polymer chain induced by the BZ reaction, since the amount of polymer aggregation is larger in the oxidized state than in the reduced state, which leads to changes in transmittance due to changes in the light scattering from the aggregated polymers [49]. As shown in Figure 5, the baseline of the self-oscillation gradually decreases with time

under all measurement conditions because of the sudden increase in the ionic strength of the solution when the measurements start [39,40]. In order to start the aggregation-disaggregation self-oscillation of the polymer chain, the polymer solution and the other BZ substrate solutions (HNO_3, MA, and $NaBrO_3$ solutions) are mixed just before the measurements. The ionic strength significantly affects the solubility of the polymer chain, and in general, solutions with high ionic strengths decrease the solubility. Because the BZ reaction requires a high concentration of the BZ substrates and thus a high ionic strength, the solubility of the polymer chain suddenly decreases at beginning of the transmittance measurements. Furthermore, the width of the waveforms for the transmittance self-oscillation decreases with increasing [MA]. The period of the transmittance self-oscillation is synchronized with the BZ reaction because the polymer aggregation sates depend on the redox state of the metal catalyst moiety. As the concentration of the solution including BZ substrates increases, the period decreases. Therefore, the width of the waveform decreases with increasing concentration of the BZ substrates [40].

Figure 5. Oscillating transmittance profiles at 14 ℃ for 0.5 wt% poly(VP-*co*-Ru(bpy)$_3$) solution at fixed nitric acid and sodium bromate conditions ($[HNO_3]$ = 0.3 M and $[NaBrO_3]$ = 0.3 M) and with (**A**) [MA] = 0.04 M, (**B**) [MA] = 0.05 M, (**C**) [MA] = 0.06 M, (**D**) [MA] = 0.07 M, (**E**) [MA] = 0.08 M, and (**F**) [MA] = 0.09 M.
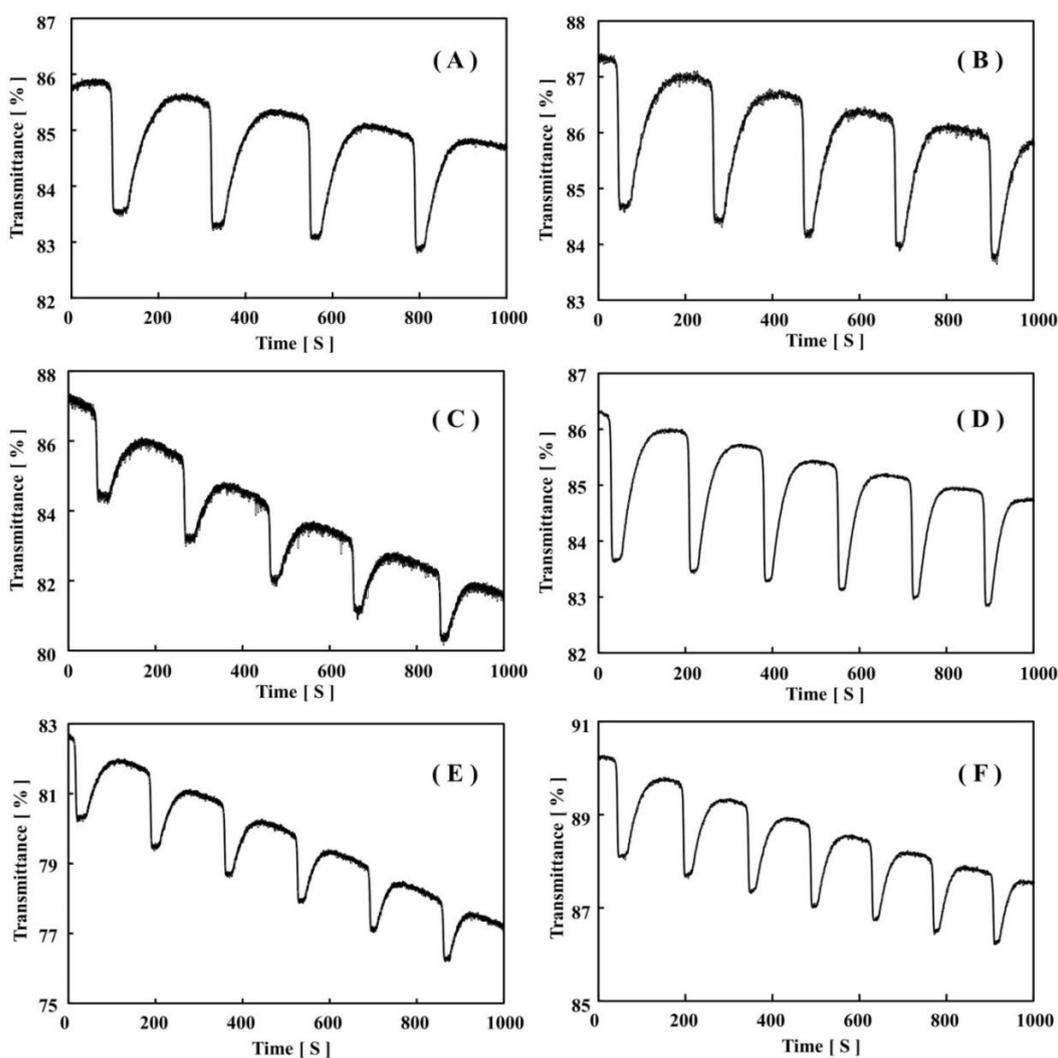
Figure 6 shows the amplitude of the aggregation-disaggregation self-oscillation for BZ substrate concentrations at 14 ℃. As shown in Figure 6, the amplitudes of the self-oscillation for the VP-based polymer chain are almost the same and are hardly influenced by the initial concentration of the BZ substrate. In contrast, for the NIPAAm-based self-oscillating polymer chain, the concentrations of the BZ substrates significantly affect the self-oscillating behavior [39,40]. Thus, we can control the self-oscillating behavior by selecting an appropriate molecular structure of the polymer main chain.

Figure 6. Dependence of the amplitude of the transmittance self-oscillation of the polymer solution at 14 ℃ for different Belousov-Zhabotinsky (BZ) substrate concentrations: [MA] = 0.04, 0.05, 0.06, 0.07, 0.08, and 0.09 M for fixed [NaBrO$_3$] = 0.3 M and [HNO$_3$] = 0.3 M); [NaBrO$_3$] = 0.1, 0.2, 0.3, 0.4, 0.5, and 0.6 M for fixed [MA] = 0.1 M and [HNO$_3$] = 0.3 M; and [HNO$_3$] = 0.1, 0.2, 0.3, 0.4, 0.5, and 0.6 M for fixed [NaBrO$_3$] = 0.1 M and [HNO$_3$] = 0.3 M.
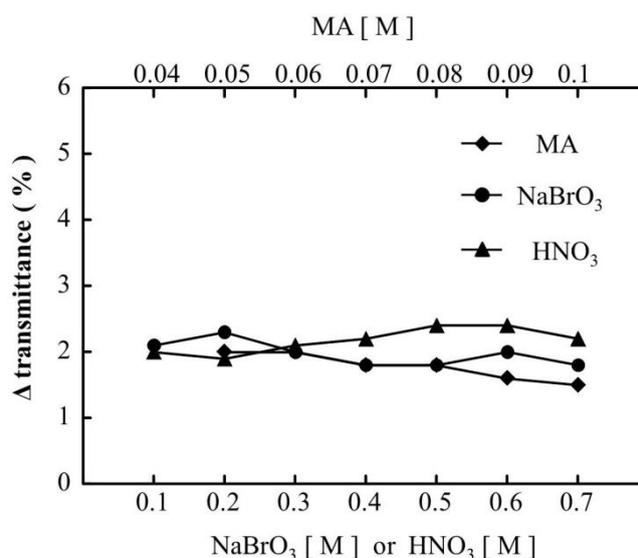

Figure 7 shows that all the logarithmic plots of the period of the self-oscillation of the VP-based polymer as a function of the initial molar concentration of one BZ substrate chain show good linear relationships [49]. Therefore, the period [T(s)] of the self-oscillation can be expressed as a[substrate]^b where a and b are experimental constants and brackets denote the initial concentration. As shown in Figure 7C, there is the saturation point. In addition, for all experimental conditions, the self-oscillation period shows a different trend compared to that observed for the NIPAAm-based polymer gel [56], where the period increases as the concentration of nitric acid increases. In general, the period of the BZ reaction decreases as the concentration of the BZ substrate increases, so the trend observed VP-based polymer is considered more natural.

Figure 8 shows the effect of the polymer concentration on the period of the transmittance self-oscillation at fixed concentrations of all three BZ substrates at 20 ℃ [51]. The viscosity of the polymer solution increases with increasing polymer concentration. As the polymer concentration increases, the number of Ru(bpy)$_3$ groups increases. The diffusion constant of the BZ substrates decreases with increasing polymer concentration, so the period of the self-oscillation hardly changes with increase in the number of Ru(bpy)$_3$ moiety.

Figure 7. Logarithmic plots of period *T* (in s) *vs.* initial molar concentration of one BZ substrate at a constant temperature (*T* = 20 ℃) under fixed concentrations for the other two BZ substrates: (**A**) [NaBrO$_3$] = 0.3 M and [HNO$_3$] = 0.3 M, (**B**) [MA] = 0.1 M and [HNO$_3$] = 0.3 M, and (**C**) [MA] = 0.1 M and [NaBrO$_3$] = 0.3 M.
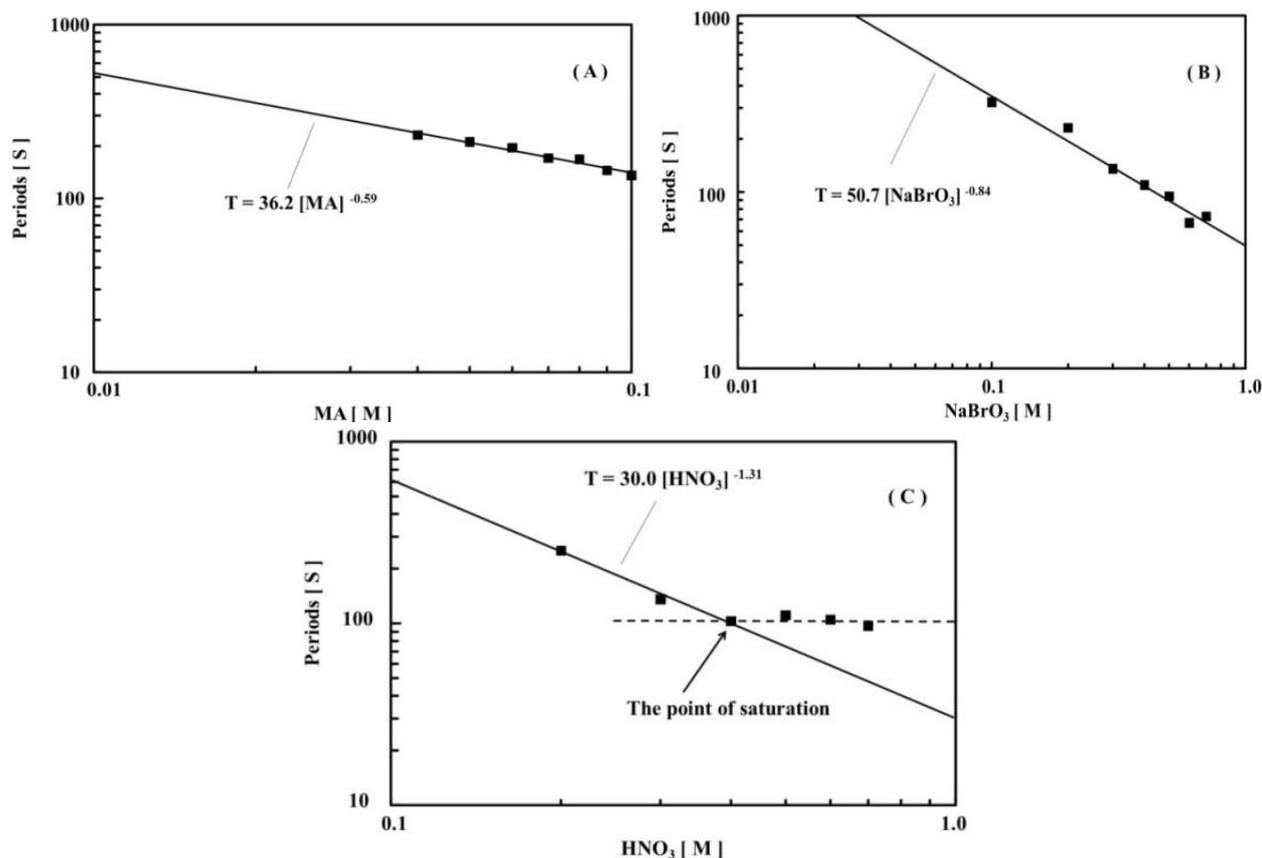
Figure 8. Dependence of self-oscillation period on concentration of poly(VP-*co*-Ru(bpy)$_3$) solution under fixed concentrations of the three BZ substrates ([MA] = 0.0625 M and [HNO$_3$] = 0.3 M, [NaBrO$_3$] = 0.084 M) at 20 ℃.

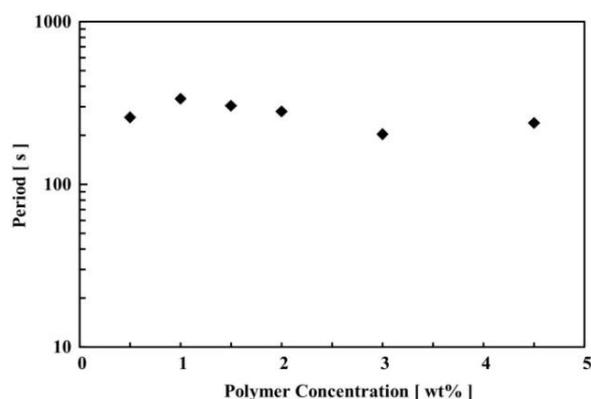Figure 9A–C shows the Arrhenius dependence of the oscillating frequency on the temperature (20–44 ℃) in a wide concentration rage of the three BZ substrates [52]. The period and temperature have a good linear relationship, which demonstrates that the period of the self-oscillation of the VP-based polymer chain follows the Arrhenius equation. Figure 9D shows the dependence of

activation energies of the VP-based polymer chain on the concentrations of three BZ substrates, where three characteristic behaviors can be observed. First, the activation energy is hardly affected by the concentrations of the three BZ substrates. Second, the activation energy is almost the same as that of the NIPAAm-based self-oscillating polymer gel below the LCST [57]. Finally, the activation energy of the self-oscillating polymer system is almost the same as that of the normal BZ reaction, *i.e.*, the reaction not including the self-oscillating polymer system with the Ru moiety [58].

Figure 9. Arrhenius dependence of oscillating frequency, F*osc*, on temperature for different concentrations of one BZ substrate under fixed concentrations of the other two BZ substrates: (**a**) [MA] = 0.1 M and [HNO$_3$] = 0.3 M, (**b**) [NaBrO$_3$] = 0.3 M and [HNO$_3$] = 0.3 M, and (**c**) [NaBrO$_3$] = 0.3 M and [MA] = 0.1 M. (**d**) Dependence of activation energy on concentrations of the three BZ substrates.
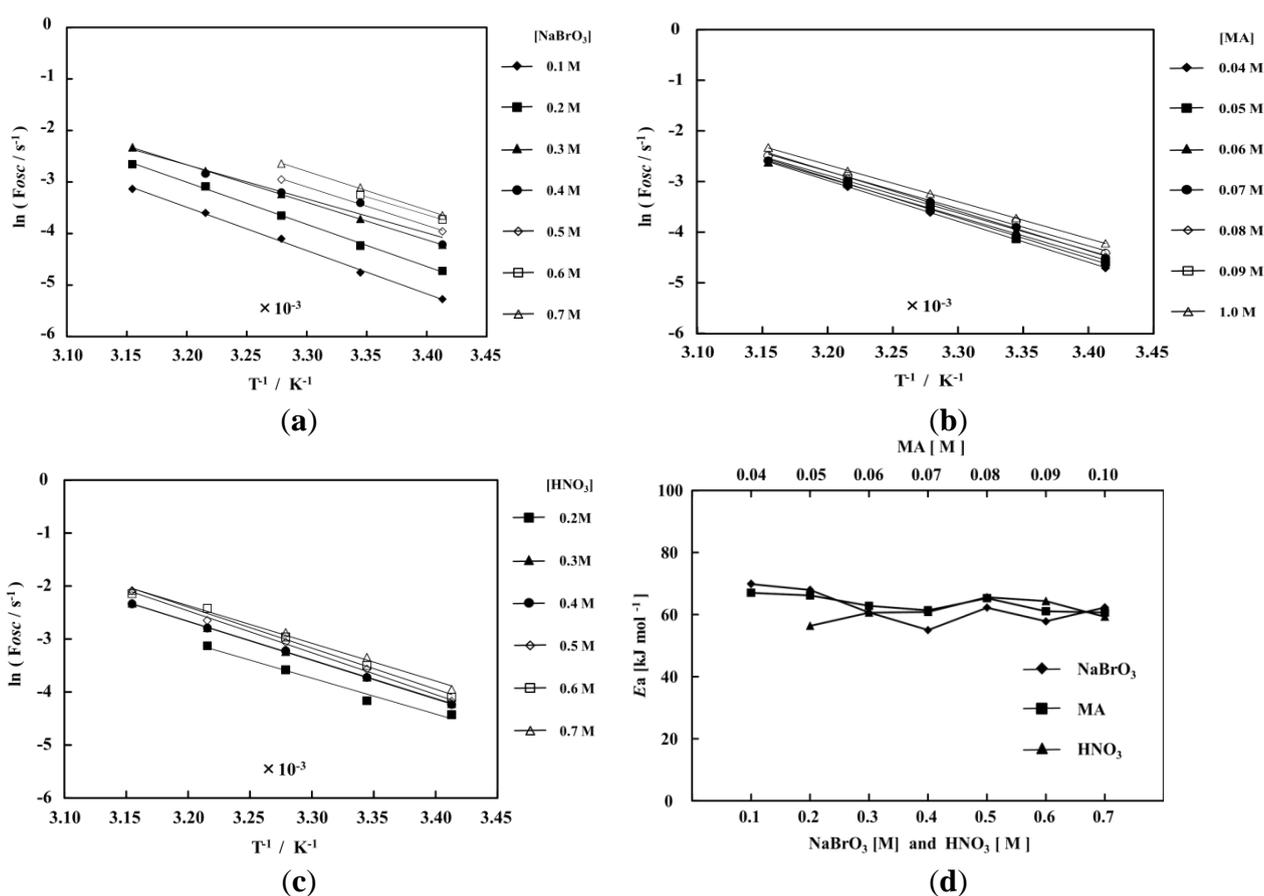
The equilibrium swelling ratios of the poly(VP-*co*-Ru(bpy)$_3$) gel in the reduced and oxidized states are shown in the Figure 10 [48]. No volume phase transitions are observed in either state because the volume of the VP-based polymer gel is not affected by the temperature. The equilibrium swelling ratio of the VP-based polymer gel in the oxidized state is larger than that in the reduced state, which is opposite to the behavior observed for the VP-based polymer chain. This tendency is a result of the cross-linkage structure of the gel. The driving force of the swelling-deswelling self-oscillation for the gel originates from the different solubilities of the Ru catalyst moiety in the reduced and oxidized states.

Figure 10. Equilibrium swelling ratios of poly(VP-co-Ru(bpy)$_3$) gel as a function of temperature in solutions with (●) [Ce$_2$(SO$_4$)$_3$] = 0.001 M and [HNO$_3$] = 0.3 M, and (○) [Ce(SO$_4$)$_2$] = 0.001 M and [HNO$_3$] = 0.3 M. The relative length is defined as the ratio of the characteristic diameter to that at the initial state at 20 ℃. (Reprinted from [45], Copyright American Chemical Society. Reproduced with permission.)
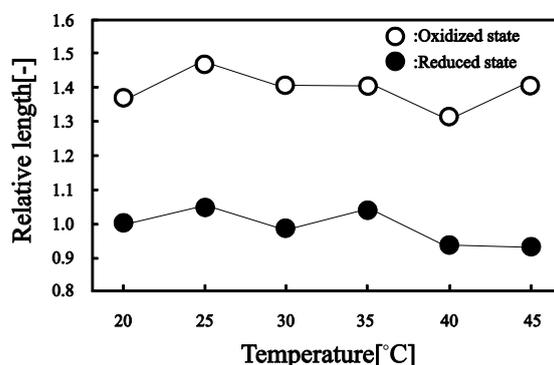
Figure 11. Logarithmic plots of period *T* (in s) *vs.* initial molar concentration of one BZ substrate at a constant temperature (*T* = 20 ℃) under fixed concentrations of the other two BZ substrates: (**a**) [NaBrO$_3$] = 0.084 M and [HNO$_3$] = 0.3 M; (**b**) [MA] = 0.0625 M and [HNO$_3$] = 0.3 M; (**c**) [MA] = 0.0625 M and [NaBrO$_3$] = 0.084M. (●) and (○) plots show the linear relation and the saturated line *vs.* initial concentration of one BZ substrate, respectively. (Reprinted from [45], Copyright American Chemical Society. Reproduced with permission.)
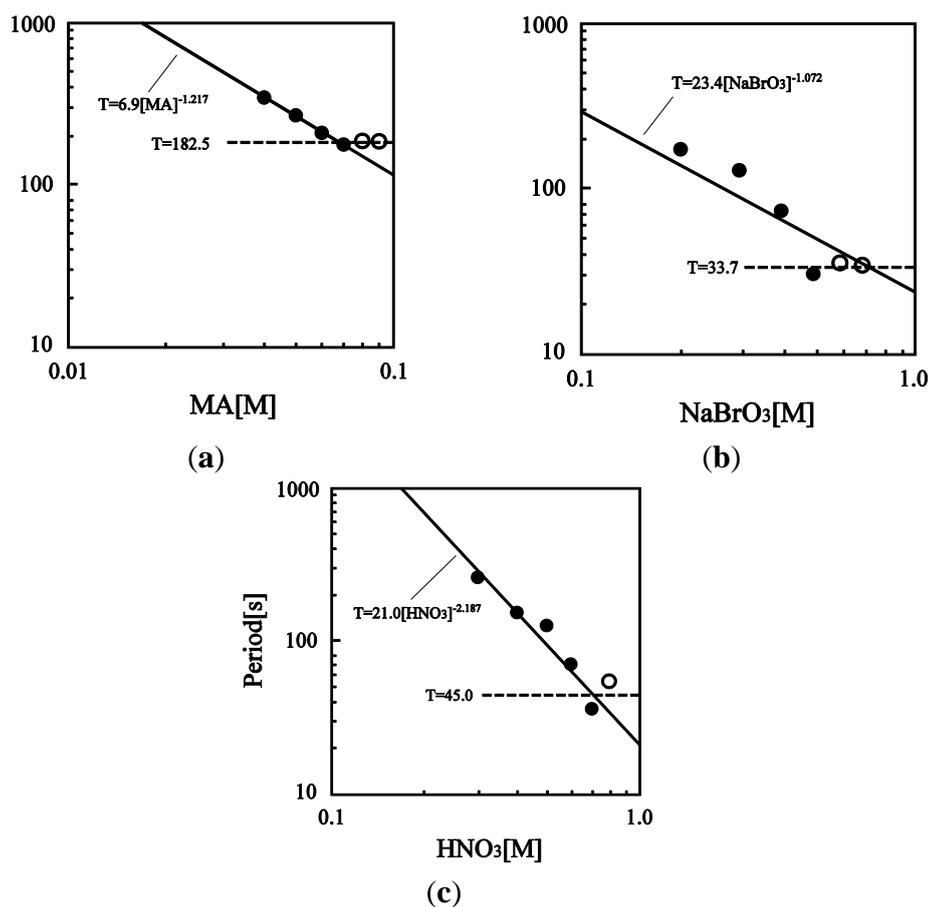

(a)

(b)

(c)

Figure 11 shows logarithmic plots of the oscillation period for the gel against the initial concentration of one BZ substrate under fixed concentrations of the other two BZ substrates at a constant temperature ($T = 20$ ℃). All the logarithmic plots show good linear relationships. Therefore, the periods [T(s)] can be expressed as a[substrate]^b where a and b are experimental constants and the brackets indicate the initial concentration. As shown in Figure 11, there are saturation points in the all logarithmic plots beyond the following initial concentrations of the BZ substrates: [MA] = 0.07 M (Figure 11a), [NaBrO$_3$] = 0.5 M (Figure 11b), and [HNO$_3$] = 0.7 M (Figure 11c). The period of the saturation point in Figure 11a is higher than that in Figure 11b,c, because of the higher mole fraction of the reduced Ru(bpy)$_3$ moiety in the gel [48]. In addition, at [MA] = 0.0625 M and [NaBrO$_3$] = 0.084 M (Figure 11c), the period can be changed by changing the initial concentration of the HNO$_3$ over a much wider range for the VP-based gel than for the poly(NIPAAm-*co*-Ru(bpy)$_3$) gel [59].

Figure 12. (**a**) Dependence of the self-oscillation period on the temperature. Filled (●) and open (○) circles show the linear relation and the saturated line *vs.* temperature, respectively. (**b**) Self-oscillating profile of cubic poly(VP-co-Ru(bpy)$_3$) gel at 50 ℃ ([MA] = 0.08 M, [NaBrO$_3$] = 0.48 M, and [HNO$_3$] = 0.48 M). (**c**) Self-oscillating profile of cubic poly(VP-co-Ru(bpy)$_3$) gel at 20 ℃ ([MA] = 0.08 M, [NaBrO$_3$] = 0.48 M, and [HNO$_3$] = 0.48 M). The cubic gel (side lengths of about 2 mm and 20 mm) was immersed in 8 mL of the mixed solution of BZ substrates. (Reprinted from [45], Copyright American Chemical Society. Reproduced with permission.)

(**a**)

(**b**)

(**c**)
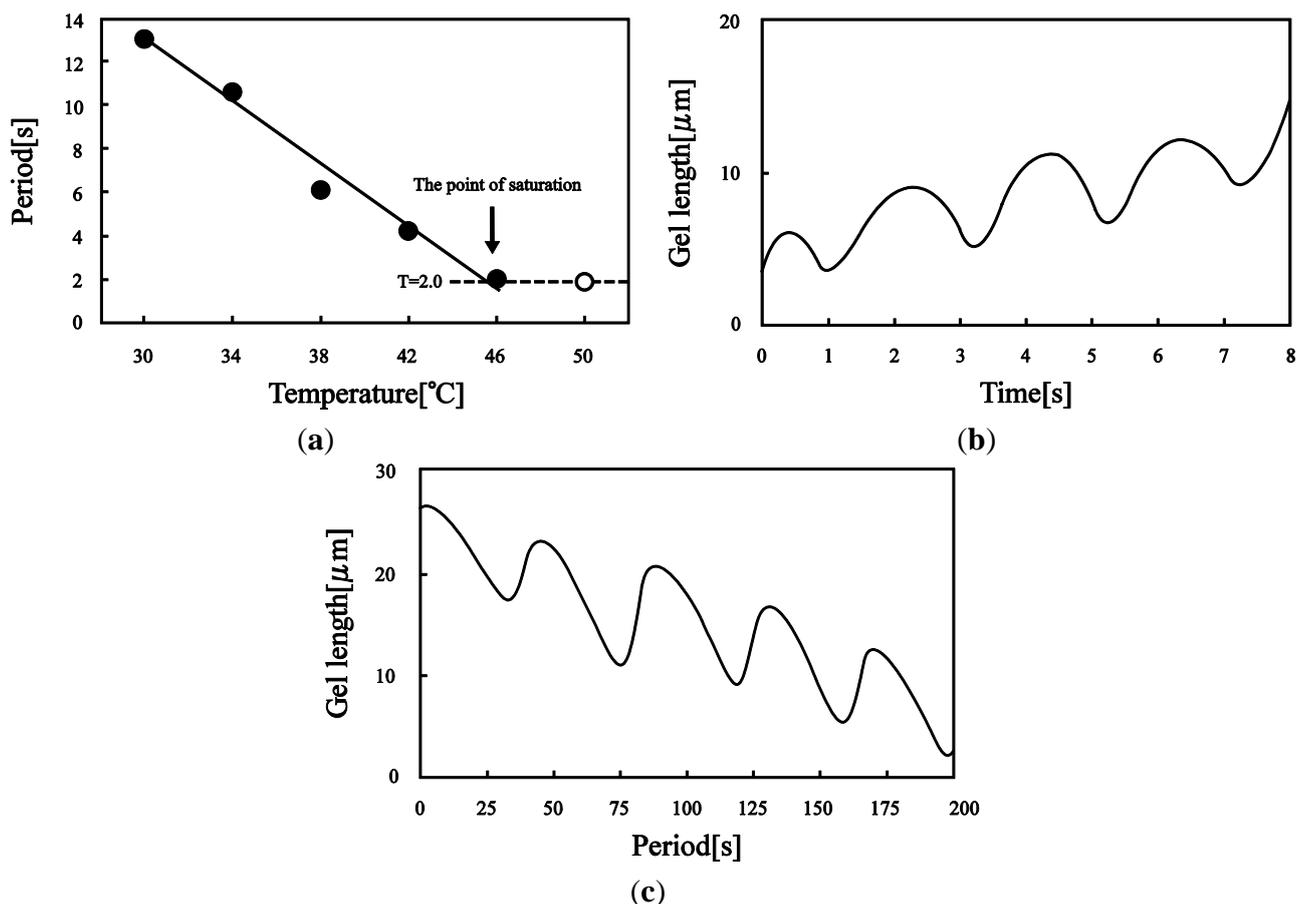
The period of the self-oscillation for the VP-based gel increases linearly with decreasing temperature, which indicates that the volume self-oscillation periods obeys the Arrhenius equation [60]. For initial concentrations [MA] = 0.08 M, [NaBrO$_3$] = 0.48 M, and [HNO$_3$] = 0.48 M at 46 ℃, the volume self-oscillation of the gel reaches a maximum period of 2 s (0.5 Hz) [48]. Thus, the maximum speed of the VP-based gel is 20 times that of the NIPAAm-based gel [56]. Figure 12b,c show the volume self-oscillation at 20 ℃ and 50 ℃, respectively. The amplitudes of the volume self-oscillation measured in terms of the length of a cubic side at 20 ℃ and 50 ℃ are 10 μm and 4 μm, respectively. These results indicate that the amplitude of the self-oscillation has a tradeoff with the period.

Figure 13. Oscillating profiles of the transmittance for the 0.5 wt% poly(AM-*co*-Ru(bpy)$_3$) polymer solutions for initial concentrations of the BZ substrates of [MA] = 0.14 M, [HNO$_3$] = 0.3 M, and [NaBrO$_3$] = 0.3 M at different temperatures: (**A**) 14 ℃, (**B**) 16 ℃, (**C**) 18 ℃, and (**D**) 20 ℃.
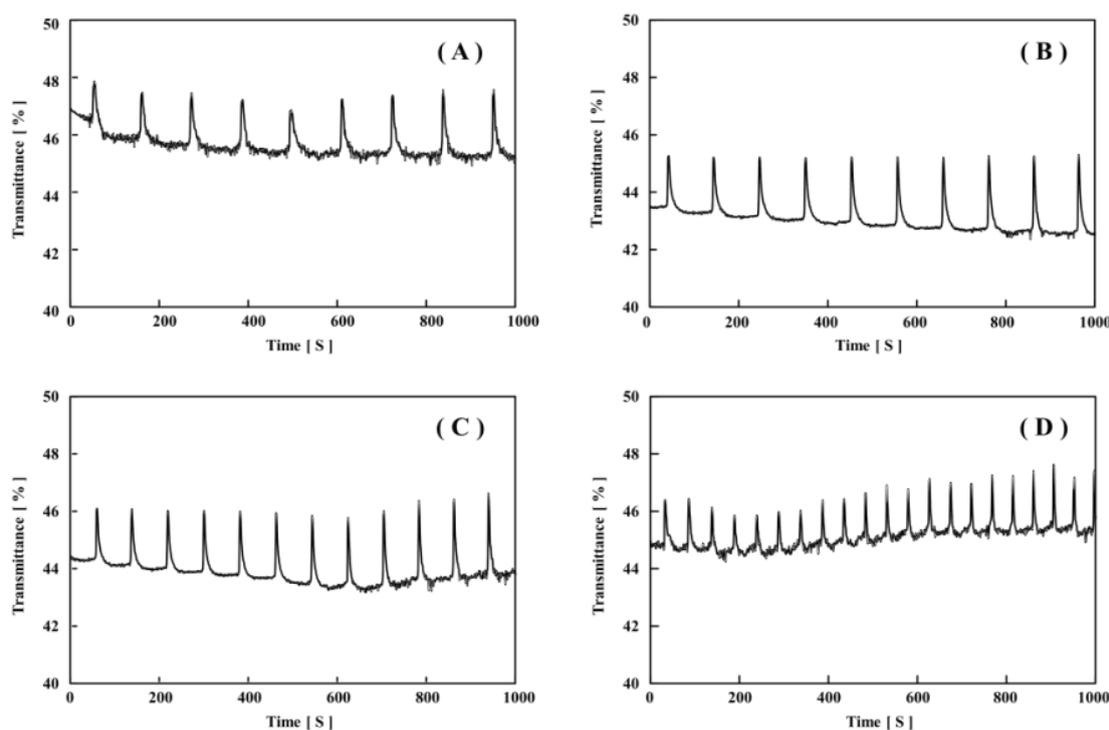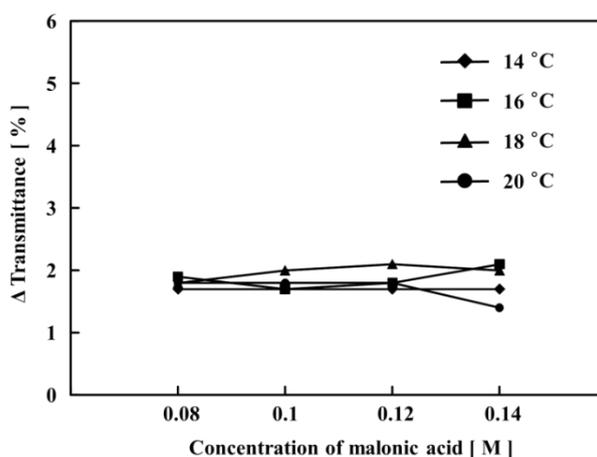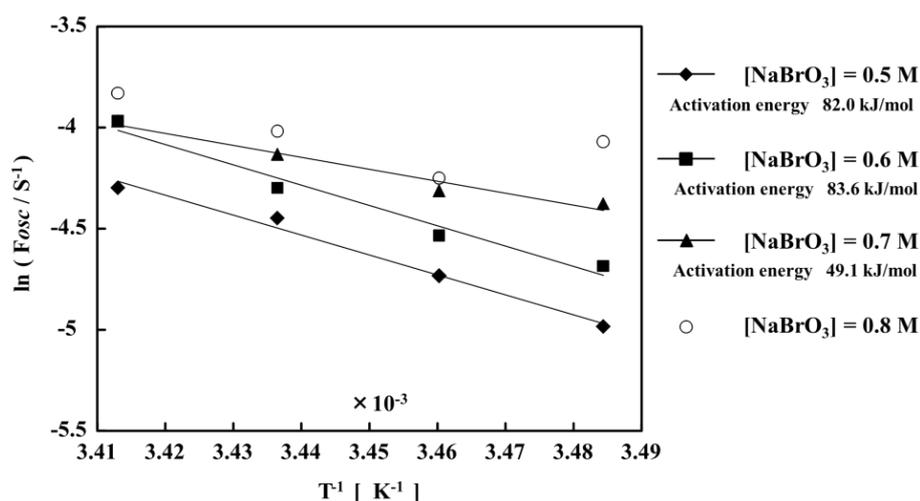

Figure 13 shows the transmittance self-oscillation for the poly(AM-*co*-Ru(bpy)$_3$) solutions at fixed concentrations of the three BZ substrates of [MA] = 0.14 M, [HNO$_3$] = 0.3 M, and [NaBrO$_3$] = 0.3 M at different temperatures of 14, 16, 18, and 20 ℃ [53]. As can be seen, the width of the transmittance self-oscillation decreases with increasing temperature because the rate of the BZ reaction increases. As with the other main chains, the transmittance self-oscillation of the AM-based polymer chain originates in the periodic changes in the solubility of the Ru catalyst moiety. The LCSTs of the poly(AM-*co*-Ru(bpy)$_3$) solution in the reduced and oxidized states were measured, but none were found because of the nonthermoresponsive nature of the AM main chain. Figure 14 shows that the amplitude of the transmittance oscillation for the AM-based polymer chain hardly changes with the malonic acid concentration [53]. In addition, the amplitude of the self-oscillation hardly changes for changes in temperature for all malonic acid conditions. This tendency is the same as was observed for the VP-based polymer chain.

Figure 15 shows that the period of the self-oscillation for the poly(AM-*co*-Ru(bpy)₃) solutions decreases with increasing temperature [55]. In addition, the period of the self-oscillation decreases with an increase in the sodium bromate concentration. From these data, the activation energy of the self-oscillation was calculated. However, at [NaBrO₃] = 0.8 M, there is no linear relationship between the period and the temperature, so the activation energy cannot be calculated. The activation energies at [NaBrO₃] = 0.5 M and 0.6 M are slightly higher than those of the VP-based polymer chain (see Figure 9D). In contrast, the activation energy at [NaBrO₃] = 0.7 M is lower than that of the VP-based polymer chain. Therefore, it is demonstrated that the activation energy of the AM-based polymer chain is significantly affected by the self-oscillating conditions.

Figure 14. Dependence of the amplitude of the transmittance self-oscillation for the poly(AM-*co*-Ru(bpy)₃) solutions on changes in the concentration of one BZ substrate ([MA] = 0.08, 0.1, 0.12 and 0.14 M) at fixed concentrations of the other two BZ substrates ([NaBrO₃] = 0.3 M and [HNO₃] = 0.3 M) at different constant temperatures (T = 14, 16, 18, and 20 ℃).

Figure 15. Period of the self-oscillation of the poly(AM-*co*-Ru(bpy)₃) polymer solution as a function of temperature (14–20 ℃) at fixed concentrations of sodium bromate and malonic acid ([NaBrO₃] = 0.3 M and [MA] = 0.1 M) and different nitric acid concentrations ([HNO₃] = 0.3, 0.4, and 0.5 M).

4. Conclusions

The influence of the initial substrate concentrations of the BZ reaction on the transmittance self-oscillation for the novel poly(VP-*co*-Ru(bpy)$_3$) solution was investigated. The amplitude of the transmittance self-oscillation was hardly affected by the initial concentrations of the BZ substrates, in contrast to the behavior observed for the NIPAAm-based polymer solution. Furthermore, the period of the transmittance self-oscillation can be controlled by selecting appropriate initial concentrations of the BZ substrates. The activation energy of the aggregation–disaggregation self-oscillation for the VP-based polymer chain was measured in a wide range of the three BZ substrate concentrations and in a wide temperature range. The activation energy of the self-oscillation is hardly affected by the concentrations of the three BZ substrates. Moreover, the activation energy of the self-oscillation is almost the same as that of the NIPAA-based self-oscillating gel below the LCST and that of the normal BZ reaction, *i.e.*, the reaction not including the self-oscillating polymer system. Details of the influence of the initial concentration of the BZ substrates and the temperature on the period of the volume self-oscillation of the poly(VP-*co*-Ru(bpy)$_3$) gel were also demonstrated. The logarithmic plots of the period against the initial concentrations of one BZ substrate with the other two BZ substrate concentrations fixed show good linear relationships. The period of the volume self-oscillation increases with increasing temperature, in accordance with the Arrhenius equation. The maximum frequency (0.5 Hz) of the poly(VP-*co*-Ru(bpy)$_3$) gel is 20 times that of the poly(NIPAAm-*co*-Ru(bpy)$_3$ gel. The amplitude of the volume self-oscillation of the gel has a tradeoff with the period of the self-oscillation. Finally, the self-oscillating behavior of the poly(AM-*co*-Ru(bpy)$_3$) was investigated. The amplitude of the self-oscillation is almost same, regardless of the temperature and the BZ substrate concentrations. The activation energy of the AM-based polymer solution is significantly affected by the self-oscillating conditions, in contrast to the behavior found for the VP-based polymer solution.

Acknowledgments

Conflicts of Interest

The authors declare no conflict of interest.

References

1. Okano, T. *Biorelated Polymers and Gels—Controlled Release and Applications in Biomedical Engineering*; Academic Press: San Diego, CA, USA, 1998.
2. Harada, A.; Kataoka, K. Chain length recognition: Core-shell supramolecular assembly from oppositely charged block copolymers. *Science* **1999**, *283*, 65–67.
3. Hoffman, A.S. Hydrogels for biomedical applications. *Adv. Drug Deliv. Rev.* **2002**, *43*, 3–12.

4. Bhattacharya, S.; Eckert, F.; Boyko, V.; Pich, A. Temperature-, pH-, and magneticfield- sensitive hybrid microgels. *Small* **2007**, *3*, 650–657.

5. Kwon, I.C.; Bae, Y.H.; Kim, S.W. Electrically credible polymer gel for controlled release of drugs. *Nature* **1991**, *354*, 291–293.

6. Chaterji, S.; Kwon, I.K.; Park, K. Hydrogels for medical and biomedical applications. *Prog. Polym. Sci.* **2007**, *32*, 1083–1122.

7. Geng, F.; Ma, R.; Nakamura, A.; Akatsuka, K.; Ebina, Y.; Yamauchi, Y.; Miyamoto, N.; Tateyama, Y.; Sasaki, T. Reversible, instant, and unusually stable ~100-fold swelling of inorganic layered materials. *Nat. Commun.* **2013**, *4*, 1632:1–1632:7.

8. Okumura, Y.; Ito, K. The polyrotaxane gel: A topological gel by figure-of-eight cross-links. *Adv. Mater.* **2001**, *13*, 485–487.

9. Kim, J.; Nayak, S.; Lyon, L.A. Bioresponsive hydrogel microlenses. *J. Am. Chem. Sci.* **2005**, *127*, 9588–9592.

10. Kwon, G.H.; Park, J.Y.; Kim, J.Y.; Frisk, M.L.; Beebe, D.J.; Lee, S.H. Biomimetic soft multifunctional miniature aquabots. *Small* **2008**, *4*, 2148–2153.

11. Seeman, N.C. Nucleic acid junctions and lattices. *J. Theor. Biol.* **1982**, *99*, 237–247.

12. Winfree, E.; Liu, F.; Wenzler, L.; Seeman, N. Design and self-assembly of two-dimensional DNA crystals. *Nature* **1998**, *394*, 539–544.

13. Yan, H.; Park, S.H.; Finkelstein, G.; Reif, J.; LaBean, T. DNA-templated self-assembly of protein arrays and highly conductive nanowires. *Science* **2003**, *301*, 1882–1884.

14. He, Y.; Chen, Y.; Liu, H.; Ribbe, A.; Mao, C. Self-assembly of hexagonal DNA two-dimensional (2D) arrays. *J. Am. Chem. Soc.* **2005**, *127*, 12202–12203.

15. Murata, S.; Konagaya, A.; Kobayashi, S.; Saito, H.; Hagiya, M. Molecular robotics: A new paradigm for artifacts. *New Gener. Comput.* **2013**, *31*, 27–45.

16. Kuzuya, Y.; Sakai, T.; Yamazaki, Y.; Xu, Y.; Komiyama, M. Nanomechanical DNA origami "single-molecule beacons" directly imaged by atomic force microscopy. *Nat. Commun.* **2011**, *2*, doi:10.1038/ncomms1452.

17. Steinberg, I.Z.; Oplatka, A.; Kachalsky, A. Mechanochemnical engines. *Nature* **1966**, *210*, 568–571.

18. Oguro, K.; Kawami, Y.; Takenaka, H. An actuator element of polyelectrotyte gel membrane-electrode composite. *Bull. Gov. Ind. Res. Inst. Osaka* **1992**, *43*, 21–24.

19. Fukushima, T.; Asaka, K.; Kosaka, A.; Aida, T. Fully plastic actuator through layer-by-layer casting with ionic-liquid-based bucky gel. *Angew. Chem. Int. Ed.* **2005**, *44*, 2410–2413.

20. Otake, M.; Kagami, Y.; Inaba, M.; Kim, B.; Inoue, H. Motion design of a starfish-shaped gel robot made of electro-active polymer gel. *Robot. Auton. Syst.* **2002**, *40*, 185–191.

21. Feinberg, A.W.; Feigel, A.; Shevkoplyas, S.S.; Sheehy, S.; Whitesides, G.M.; Parker, K.K. Muscular thin films for building actuators and powering devices. *Science* **2007**, *317*, 366–1370.

22. Ma, M.; Guo, L.; Anderson, D.G.; Langer, R. Bio-inspired polymer composite actuator and generator driven by water gradients. *Science* **2013**, *339*, 186–189.

23. Beebe, D.J.; Moore, J.S.; Bauer, J.M.; Yu, Q.; Liu, R.H.; Devadoss, C.; Jo, B.H. Functional hydrogel structures for autonomous flow control inside microfluidic channels. *Nature* **2000**, *404*, 588–590.

24. Asoh, T.; Matsusaki, M.; Kaneko, T.; Akashi, M. Fabrication of temperature-responsive bending hydrogels with a nanostructured gradient. *Adv. Mater.* **2008**, *20*, 2080–2083.

25. Ishiwatari, T.; Kawaguchi, M.; Mitsuishi, M. Oscillatry reactions in polymer systems. *J. Polym. Sci. A Polym. Chem.* **1984**, *22*, doi:10.1002/pol.1984.170221033.

26. Yoshida, R.; Sakai, T.; Ito, S.; Yamaguchi, T. Self-oscillation of polymer chains with rhythmical soluble-insoluble changes. *J. Am. Chem. Sci.* **2002**, *124*, 8095–8098.

27. Yoshida, R.; Takahashi, T.; Yamaguchi, T.; Ichijo, H. Self-oscillating gel. *J. Am. Chem. Soc.* **1996**, *118*, 5134–5135.

28. Zaikin, A.N.; Zhabotinsky, A.M. Concentration wave propagation in two-dimensional liquid-phase self-oscillating system. *Nature* **1970**, *225*, 535–537.

29. Field, R.J.; Burger, M. *Oscillations and Traveling Waves in Chemical Systems*; John Wiley & Sons: New York, NY, USA, 1985.

30. Field, R.J.; Noyes, R.M. Oscillations in chemical systems. IV. Limit cycle behavior in a model of a real chemical reaction. *J. Chem. Phys.* **1974**, *60*, 1877–1884.

31. Gyorgyi, L.; Turanyi, T.; Field, R.J. Mechanistic details of the oscillatory Belousov-Zhabotinskii reaction. *J. Chem. Phys.* **1990**, *94*, 7162–7170.

32. Turanyi, T.; Gyorgyi, L.; Field, R.J. Analysis and simplification of the GTF model of the Belousov-Zhabotinsky reaction. *J. Chem. Phys.* **1993**, *97*, 1931–1941.

33. Wood, P.M.; Ross, J. A quantitative study of chemical waves in the Belousov-Zhabotinsky reaction. *J. Chem. Phys.* **1985**, *82*, 1924:1–1924:13.

34. Tyson, J.J.; Fife, P.C. Target patterns in a realistic model of the Belousov-Zhabotinskii reaction. *J. Chem. Phys.* **1980**, *73*, 2224:1–2224:14.

35. Mori, H.; Kuramoto, Y. *Dissipative Structures and Chaos*; Springer-Verlag: Berlin, Germany, 1997.

36. Shen, J.; Pullela, S.R.; Marquez, M.; Cheng, Z. Ternary phase diagram for the Belousov-Zhabotinsky reaction-induced mechanical oscillation of intelligent PNIPAM colloids. *J. Phys. Chem. A* **2007**, *111*, 12081–12085.

37. Pullela, S.R.; Shen, J.; Marquez, M.; Cheng, Z. A comparative study of temperature dependence of induction time and oscillatory frequency in polymer-immobilized and free catalyst Belousov-Zhabotinsky reactions. *J. Polym. Sci. A. Polym. phys.* **2009**, *47*, 847–854.

38. Pullela, S.R.; Cristancho, D.; He, P.; Luo, D.; Hall, K.R.; Cheng, Z. Temperature dependence of the Oregonator model for the Belousov-Zhabotinsky reaction. *Phys. Chem. Chem. Phys.* **2009**, *11*, 4236–4243.

39. Hara, Y.; Yoshida, R. Self-oscillation of polymer chains induced by the Belousov-Zhabotinsky reaction under acid-free conditions. *J. Phys. Chem. B* **2005**, *109*, 9451–9454.

40. Hara, Y.; Yoshida, R. Damping behavior of aggregation-disaggregation self-oscillation for a polymer chain. *Marcomol. Rapid Commun.* **2009**, *30*, 1656–1662.

41. Hara, Y.; Yoshida, R. Self-oscillating polymer fueled by organic acid. *J. Phys. Chem. B* **2008**, *112*, 8427–8429.

42. Hara, Y.; Maeda, S.; Hashimoto, S.; Yoshida, R. Molecular design and functional control of novel self-oscillating polymers. *Int. J. Mol. Sci.* **2010**, *11*, 704–718.

43. Hara, Y.; Yoshida, R. Control of oscillating behavior for the self-oscillating polymer with pH-control site. *Langmuir* **2005**, *21*, 9773–9776.

44. Hara, Y.; Yoshida, R. A viscosity self-oscillation of polymer solution induced by the BZ reaction under acid-free condition. *J. Chem. Phys.* **2008**, *128*, 224904:1–224904:4.

45. Maeda, S.; Hara, Y.; Sakai, T.; Yoshida, R.; Hashimoto, S. Self-walking gel. *Adv. Mater.* **2007**, *19*, 3480–3484.

46. Maeda, S.; Hara, Y.; Yoshida, R.; Hashimoto, S. Control of the dynamic motion of a gel actuator driven by the Belousov-Zhabotinsky reaction. *Macromol. Rapid. Commun.* **2008**, *29*, 401–405.

47. Maeda, S.; Hara, Y.; Yoshida, R.; Hashimoto, S. Peristaltic motion of polymer gels. *Angew. Chem. Int. Ed.* **2008**, *47*, 6690–6693.

48. Nakamaru, S.; Maeda, S.; Hara, Y.; Hashimoto, S. Control of autonomous swelling-deswelling behavior for a polymer gel. *J. Phys. Chem. B* **2009**, *113*, 4609–4613.

49. Hara, Y.; Jahan, R.A. Influence of initial substrate concentration of the Belouzov-Zhabotinsky reaction on transmittance self-oscillation for a nonthermoresponsive polymer chain. *Polymers* **2011**, *3*, 330–339.

50. Hara, Y. Trasmittance self-oscillating behavior of a non-thermoresponsive polymer chain induced by the Belouzov-Zhabotinsky (BZ) reaction. *Key Eng. Mater.* **2011**, *480–481*, 369–374.

51. Hara, Y. Effect of substrate concentrations of the BZ reaction on period of self-oscillation for non-thermoresponsive polymer chain. *Key Eng. Mater.* **2011**, *480–481*, 357–362.

52. Hara, Y.; Jahan, R.A. Activation energy of aggregation-disaggregation self-oscillation of polymer chain. *Int. J. Mol. Sci.* **2012**, *13*, 16281–16290.

53. Hara, Y.; Jahan, R.A. Autonomous self-oscillating behavior of a novel nonthermoresponsive polymer chain. *Adv. Mater. Res.* **2012**, *429*, 46–49.

54. Hara, Y.; Jahan, R.A. Effect of concentration of nitric acid on the autonomous conformation change of a polymer chain with nonthermoresponsive nature. *Adv. Mater. Res.* **2012**, *429*, 42–45.

55. Hara, Y.; Jahan, R.A. Soluble-insoluble self-oscillation of a novel nonthermoresponsive polymer chain induced by the Belousov-Zhabotinsky reaction. *Adv. Mater. Res.* **2012**, *429*, 37–41.

56. Yoshida, R.; Onodera, S.; Yamaguchi, T.; Kokufuta, E. Aspects of the Belousov-Zhabotinsky reaction in polymer gels. *J. Phys. Chem. A* **1999**, *103*, 8573–8578.

57. Miyakawa, K.; Sakamoto, F.; Yoshida, R.; Yamaguchi, T.; Kokufuta, E. Chemical waves in self-oscillating gels. *Phys. Rev. E* **2000**, *62*, 793–798.

58. Kuhnert, L.; Krug, H.J. Kinetics of chemical waves in the acidic bromate-malonic acid-tris(bipyridine)ruthenium(2+) system in comparison with the ferroin system. *J. Phys. Chem.* **1987**, *91*, 730–733.

59. Yoshida, R.; Tanaka, M.; Onodera, S.; Yamaguchi, T.; Kokufuda, E. In-phase synchronization of chemical and mechanical oscillations in self-oscillating gels. *J. Phys. Chem. A* **2000**, *104*, 7549–7555.

60. Yoshikawa, K. Distinct activation energies for temporal and spatial oscillations in the Belousov-Zhabotinskii reaction. *Bull. Chem. Soc. Jpn.* **1982**, *55*, 2042–2045.